VELOCITY CORRELATION SCALES IN THE WAKE OF A WIND TURBINE

Lorenn Le Turnier
Max Planck Institute
for Dynamics and Self-Organization
Georg-August-Universität Göttingen
Göttingen, Germany
lorenn.le-turnier@ds.mpg.de

Hyunseok Kim
Max Planck Institute
for Dynamics and Self-Organization
Göttingen, Germany
hyunseok.kim@ds.mpg.de

Jan Moláček
Max Planck Institute
for Dynamics and Self-Organization
Göttingen, Germany
jan.molacek@ds.mpg.de

Christian Küchler
Max Planck Institute
for Dynamics and Self-Organization
Göttingen, Germany
christian.kuechler@ds.mpg.de

Eberhard Bodenschatz
Max Planck Institute
for Dynamics and Self-Organization
Georg-August-Universität Göttingen
Göttingen, Germany
eberhard.bodenschatz@ds.mpg.de

Claudia E. Brunner
Technical University of Munich
Munich, Germany
Max Planck Institute
for Dynamics and Self-Organization
Göttingen, Germany
c.e.brunner@tum.de

ABSTRACT

Understanding the turbulent dynamics of wind turbine wakes is crucial for predicting turbine-turbine interactions in wind farms. Here we investigate the spatial development of velocity correlation functions in a wind turbine wake in order to understand what spatial scales dominate the turbulence in different regions of the wake. We do this by analysing Lagrangian particle tracking data acquired in the wake of a model wind turbine with a diameter-based Reynolds number of $Re_D = 1 \times 10^6$. The three-dimensional, time-resolved nature of the particle tracking data enables the computation of spatially resolved velocity correlation functions of all velocity components. Here, we study the radial correlation functions of the azimuthal velocity component. Wake data were recorded up to five diameters downstream. The two-point one-time velocity correlations of particle pairs in the core wake, the shear layer and the outer wake region are studied as a function of downstream position. They reveal coherent structures being injected into the core at size smaller than half the rotor. As the wake develops downstream, the correlation of the core wake, the shear layer and the outer wake converge towards a similar profile, consistent with the mixing induced by the expansion of the shear layer. The present results demonstrate the potential of the two-point one-time radial correlation of the azimuthal velocity component to characterise the evolution of coherent structures throughout the wind turbine wake.

INTRODUCTION

In wind farms, front row turbines produce more electricity than downstream turbines. This is because downstream turbines are affected by the turbulent wakes of upstream turbines (Porté-Agel *et al.* (2020)). Because the turbulence is responsible for momentum entrainment from the freestream, an accurate understanding of the turbulence in different parts of the wake is necessary to accurately predict wake recovery.

The turbulence present in wind turbine wakes originates from inflow turbulence, from the shear layer between the wake and the freestream and from the breakdown of the tip, root and hub vortices. This leads to a highly inhomogeneous, anisotropic flow that continues to develop many diameters downstream. Neunaber *et al.* (2020) used hot wire anemometry to study a wind turbine wake and were able to identify four downstream turbulence regions within the wake, regardless of the inflow conditions. The near wake region close to the turbine is characterised by high levels of small-scale turbulence due to the hub and root vortices being shed from the center of the rotor. These vortices are unstable and quickly break down, generating turbulence. In the transition zone, the tip vortices break down, generating regions of high intermittency. This triggers the transport of smaller scale turbulence into the wake core as the shear layer expands. In the decay zone, the shear layer that surrounds the wake has already merged in the center. The integral scale increases as larger-scale turbulent structures are transported into the wake. Finally, the wake turbulence converges to fully homogeneous isotropic turbulence.

Velocity correlation functions show over which spatial scales turbulent fluctuations are correlated in a flow and thus reveal which scales dominate the flow. They are therefore well suited to characterise the presence of large-scale structures in a wind turbine wake. However, to the authors' knowledge, spatial velocity correlations have rarely been studied in this context. Placidi *et al.* (2023) investigated the influence of atmospheric thermal stability on turbulence length scales in a wind turbine wake by computing two-point correlations of all three velocity components using two laser Doppler anemometry (LDA) probes. This study demonstrated that two-point correlations provides a way to identify organized coherent structures in the flow and to quantify their characteristic spatial dimensions.

The approach of computing velocity correlation functions from Lagrangian particle tracking (LPT) data remains largely unexplored. It has traditionally been extremely challenging to acquire time-resolved, three-dimensional, three-component velocity information in a turbulent flow. Recent advances in experimental and computational capabilities have made Lagrangian particle tracking possible at relatively high particle densities, allowing this technique to yield valuable insight into inhomogeneous, anisotropic flows.

In the present work, the two-point one-time velocity correlation between particle pairs is investigated to characterise the dominant spatial structures in a wind turbine wake. The azimuthal velocity component u_θ is of particular interest in the near-to-mid wake region, where the rotor injects angular momentum into the flow and generates the rotating, helical wake described above. In this study, we address the following question:

- Can the velocity correlation capture the downstream evolution of these structures, their breakdown and the mixing driven by the shear layer expansion?

Using LPT measurements, we are able to reconstruct the three-dimensional flow up over $0 \leq D \leq 4.8$ diameters downstream of the rotor. We first introduce the facility and the experimental methodology used for this work. We then present the results and suggest future work.

EXPERIMENTAL SETUP

The Variable Density Turbulence Tunnel

The experiments are conducted in the Variable Density Turbulence Tunnel (VDTT) at the Max Planck Institute for Dynamics and Self-Organization (MPI-DS) (Bodenschatz *et al.* (2014), see Figure 1).

The present experiment is conducted in the upper test section of the wind tunnel, which is 8.8 m long with a cross-sectional area of 1.7 m^2. The wind tunnel is filled with sulphur hexafluoride (SF_6) and pressurized up to 15 bar in order to achieve diameter-based Reynolds numbers of $Re_D = \rho U_\infty D/\mu \sim 10^6$, where ρ is the density, U_∞ the mean velocity and μ the dynamic viscosity of the flow. The gas can be circulated at up to 5 m/s by a fan located in the lower section of the tunnel. In this study, a slow mean inflow velocity was used in order to have longer trajectories, leading to a diameter-based Reynolds number of $Re_D \approx 1 \times 10^6$ at a 6bar pressure. The summary of the inflow conditions is detailed in table 1.
The experiment is realized with open-grid inflow condition as a canonical case.

The wind turbine model

The wind turbine model used for this study has a V27 rotor with a diameter of $D = 16$ cm and was adapted from Miller *et al.* (2019). A motor has been integrated to actively control the rotation speed of the turbine. The rotation speed of the turbine is set to reach a constant tip speed ratio (TSR) value over the experiments where $TSR = \frac{\omega(D/2)}{U_\infty}$ which measured how fast the wind turbine rotates at the blade tip compared to the mean inflow velocity. To determine the correct motor speed, we used a measuring laser mounted on the traverse as a first estimation (see figure 1) and then manually measured the real rotation using the camera frames. During the measurements, the laser was moved on the very right end of the wind tunnel to not disturb the wake. However, to control the consistency of the rotation, we moved back the laser after some runs to measure the frequency. On figure 2 (right) is represented the rotation frequency measured by the laser for a sample of the data. We see that the rotation frequency stayed mostly constant around 24.43Hz over the different runs.

The wind turbine is mounted on a linear axis system which can be moved horizontally. Therefore, while the measurement volume is fixed in space, the turbine can be moved relative to the volume in order to study various parts of the flow around the turbine, from the inflow to the far wake.

Lagrangian Particle Tracking Setup

To study the three-dimensionality of spatial structures in the wind turbine wake, we use a Lagrangian particle tracking setup adapted from Küchler *et al.* (2024): tracer particles are injected into the upstream flow, illuminated as they pass through the measurement volume and recorded by cameras from four different perspectives, allowing for the reconstruction of the three-dimensional particle tracks. For particles to act as perfect tracers in a turbulent flow, they must be neutrally buoyant and smaller than the Kolmogorov length scale. This is characterized by the Stokes number, which must be $St \leq 0.1$. In highly turbulent flows, this is extremely challenging to achieve. Here, hollow (air-filled) glass spheres with an average diameter of 65μm were used as tracers. At 6bar SF_6, the particles have a positive buoyancy. However, the low level of turbulence of this experiment results in a large Kolmogorov timescale of SF_6, yielding a Stokes number in the order of 10^{-1}.

The particle injection system consists of a small reservoir filled with the glass bubble particles located under the floor inside the test section. High pressure SF_6 is injected inside the reservoir where the pressure difference with the wind tunnel pressure is $\Delta p = 2bar$. The particles are ejected through an outlet pipe located in the middle of the test section and disperse sufficiently by the time they enter the measurement volume (see figure 1). The particle density is entirely determined by the injection system which is then only controlled by the pressure injected and the duration of this injection therefore, the resulting particle density is never consistent for every runs. For this reason, it was difficult to get many particles less than 5mm separation from each other. The glass bubble particles are illuminated by four LEDs (Cree LMH2) mounted in the tunnel wall. Four Phantom T4040 high-speed cameras are mounted below the test section and record the displacement of the particles from different angles at a frame rate of 5kHz. The resulting measurement volume is determined by the size of the particles and the resolution of the cameras, in this case 2560×1664 pixels. We obtained a measurement volume size of $V = 13 \times 17 \times 15$ cm^3. When accumulating all trajectories from the different positions, we were able to record trajectories up to 4.8D downstream the wind turbine.

The resulting images are then post-processed and the three-dimensional trajectories of the particles are obtained using an in-house Shake-the-box code Bertens *et al.* (2021).

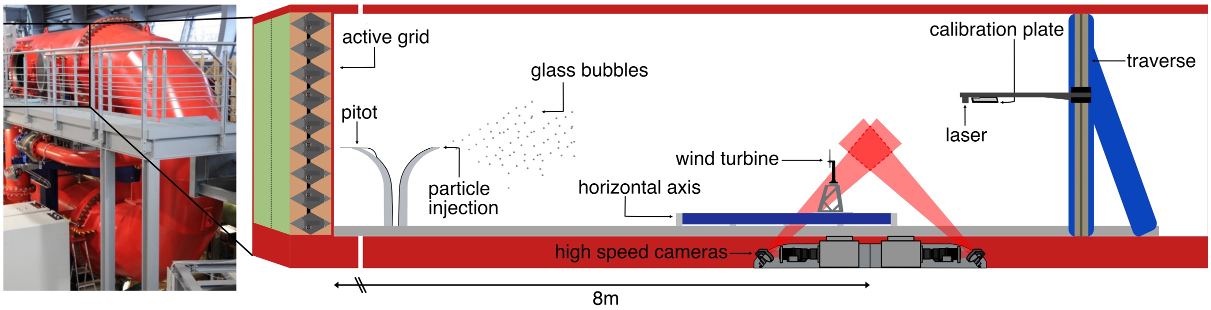

Figure 1. (Left) Picture of the Variable Density Turbulence Tunnel (VDTT). (Right) Schematic of the upper section of the VDTT and the Lagrangian Particle Tracking setup.

Table 1. Experimental conditions. U_∞ is obtained with Pitot measurements at the entrance of the test section.

Grid protocol	Fluid	Pressure [bar]	ρ $[kg/m^3]$	ν [Pa.s]	U_∞ [m/s]	Re_D	TSR
Open grid	SF_6	6	38.857	1.51×10^{-5}	2.47	1.02×10^{6}	5

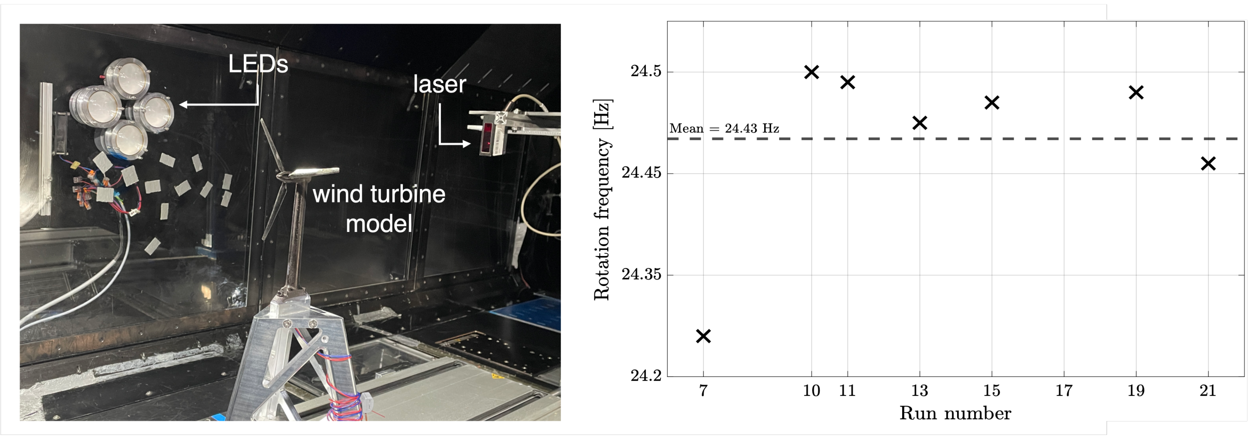

Figure 2. (Left) Picture of the wind turbine model. (Right) Rotation frequency of the wind turbine model for different data, measured by the laser visible on the left picture. The mean rotation frequency of all runs is $24.4259Hz$.

To obtained the statistics of velocity of the Lagrangian trajectories, the tracks are derived using penalized splines (Lawson *et al.* (2018)). This method was found to introduce less bias in data compared to other methods.

METHODOLOGY

The particle velocities are used to compute the two-point one-time radial velocity correlation of the azimuthal velocity component between particle pairs as a function of their radial separation. Figure 3 represents the measurement domain and is used to explain our methodology: the wake is represented in cylindrical coordinates $[X,R,\theta]$, with X is the streamwise coordinate measured from the rotor plane, R is the radial coordinate measured from the rotor axis and θ is the azimuthal angle in the rotor cross-sectional plane, measured from the horizontal. The velocity correlation is analyzed at three radial regions: the core wake $R/D\in[0.0,0.4[$, the shear layer $R/D\in[0.4,0.6]$ and the outer wake $R/D>0.6$. The wake is divided into successive streamwise slices, chosen to be wide enough to satisfy convergence while still spatially resolving the wind turbine wake. The slice width is set to $\Delta X/D=0.4$ (see figure 3).

We consider particle A visible at time t_A and particle B its paired particle. To make sure the particle A and B are closely aligned in the streamwise and azimuthal directions, we compute the ratio of their streamwise and azimuthal separations to the radial separation between the two particles:

$$\varepsilon=\frac{\sqrt{(R\times\Delta\theta)^2+(\Delta X)^2}}{\Delta R} \tag{1}$$

where $[\Delta X,\Delta R,\Delta\theta]$ are respectively the streamwise, radial and azimuthal separations between the two particles, and R is the radial coordinate of particle A. Particle B is a valid pair for particle A if ε is small enough. The two-point one-time radial correlation of the azimuthal velocity component can be written as:

$$\rho_{u_\theta}(\Delta R)=\frac{<u'_{\theta_A}\times u'_{\theta_B}>}{\sqrt{<u'^2_{\theta_B}><u'^2_{\theta_A}>}} \tag{2}$$

Figure 4 shows the effect of ε threshold on the velocity correlation at downstream position $X/D\in[0.4,0.8]$, for the core wake, the shear layer and the outer wake. While the outer

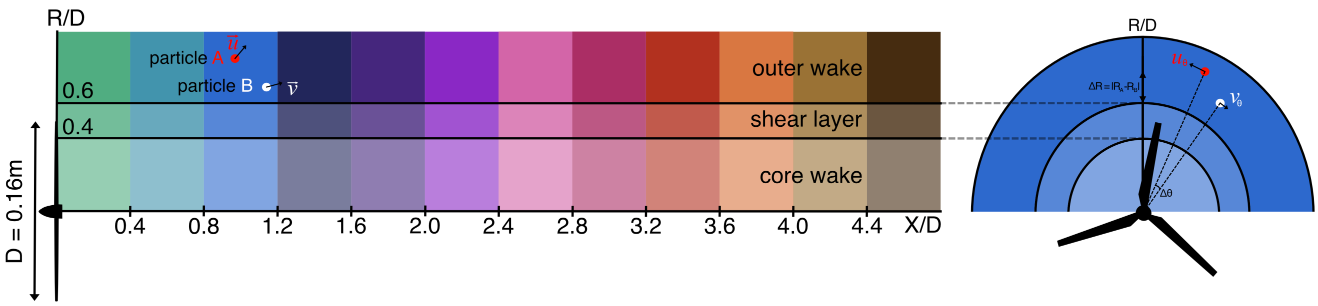

Figure 3. (Left) Schematic of the wind turbine wake in side view and (right) front view. The colored slices in the side view indicate the streamwise slices used for the radial correlation, covering $X/D \in [0, 4.8]$. The front view shows the three radial regions: the core wake ($R/D \in [0, 0.4[$), the shear layer ($R/D \in [0.4, 0.6]$) and the outer wake ($R/D > 0.6$).

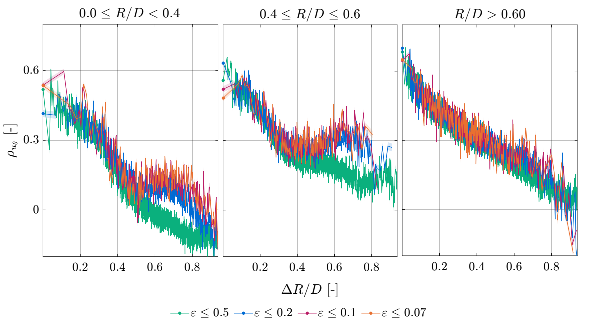

Figure 4. Two-point one-time azimuthal velocity correlation ρ_{u_θ} at $X/D \in [0.4, 0.8]$ for varying ε threshold.

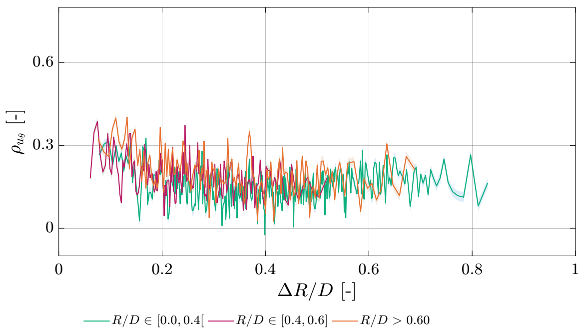

Figure 5. Two-point one-time correlation of the rotational velocity component ρ_{u_θ} as a function of the radial separation $\Delta R/D$ measured in the inflow.

wake shows no significant dependence on ε, the velocity correlation in the core wake and in the shear layer converges for $\varepsilon \leq 0.1$ which is therefore chosen for the rest of the analyses. Additionally, the resolution is reduces at the smallest and largest separations, where the bin width is larger. These regions will be excluded for the rest of the study.

The final two-point one-time radial correlation of the azimuthal velocity component is obtained by binning particle-pair correlations by radial separations ΔR and averaging within each bin. A convergence study was conducted on the number of particle-pairs per bin (not show): a minimum of 3000 particle-pairs per bin is adopted for the entire study. Furthermore, slices containing fewer than 30 data points were excluded from the analysis to ensure sufficient resolution to capture the correlation scales without artificially smoothing smaller-scale features.

After the convergence analysis, the correlation profiles remain scattered. A moving average is therefore applied to characterize the evolution of the correlation scales in the wake as a function of downstream position and to avoid misinterpreting statistical fluctuations. For the rest of this study, we define L_0 as the separation at which the smoothed velocity correlation function crosses zero for the first time.

RESULTS

As discussed previously, the number of data points acquired for small separations was generally insufficient to reach statistical convergence at these scales. Therefore the correlation functions do not extend to very small separations. However, statistical convergence was achieved for the scales of interest in this study, ranging from the chord length to the rotor diameter.

First, we investigate the correlation in the inflow where radial homogeneity is known a priori. Figure 5 shows the radial two-point one-time correlation of the rotational velocity component for the radial flow region upstream of the core wake, shear layer and outer wake. As expected, no dependence on radial region is observed in the homogeneous inflow, validating the methodology. The fact that the correlation functions do not consistently reach zero suggests that the integral length scale in the inflow is larger than the field of view in our experiment.

Figure 6 shows the radial correlation functions of the rotational velocity component for the core wake, shear layer and outer wake. Results are presented at successive downstream positions X/D in the wake, as defined in figure 3.

Core wake In the near wake, the correlation is strong at smaller separations, but decreases steeply up to $\Delta R/D = 0.5$ and then remains constant at a low positive value for larger separations. It crosses zero around $L_0 = 0.9D$. Over $X/D = [0.4, 1.6]$, the strength of the small-scale correlation and the extent of this correlated scale range decreases from $\Delta R/D = 0.5$ to 0.3 while L_0 remains constant. Directly behind the rotor, the dominant length scale in the core wake region is on the order of the rotor radius, meaning that the wake flow is mostly governed by the rotor rotation. Neunaber *et al.* (2020) have shown that this region is associated a reduction in turbulent length scales. The high correlations at small separations may be associated with the hub vortex. As the flow convects down-

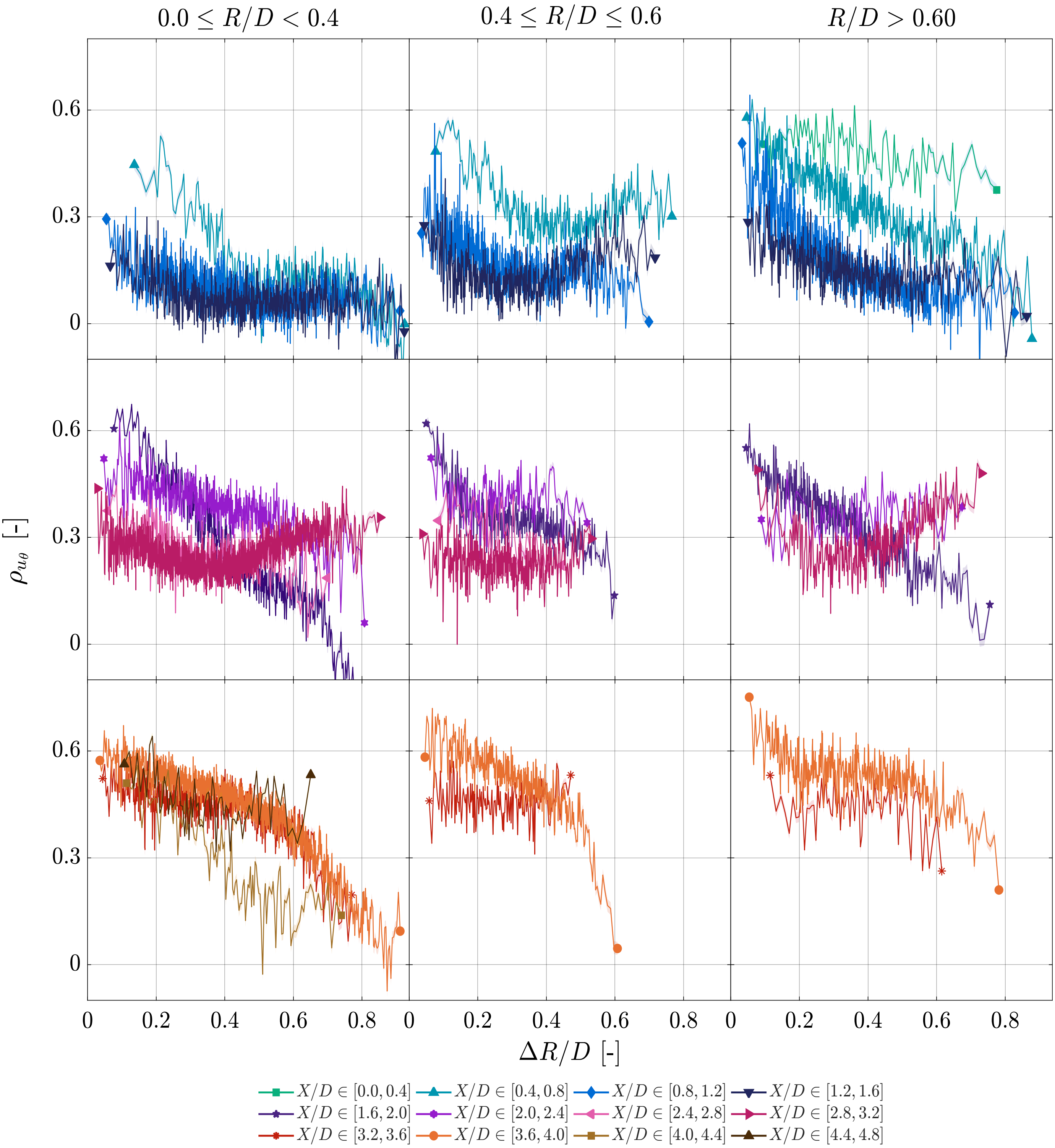

Figure 6. Two-point one-time azimuthal velocity correlation ρ_{u_θ} between particle-pairs as a function of their radial separation ΔR.

stream, the vortex structures break down, which enhances mixing across all scales and may explain the observed decrease in correlation.

At $X/D \in [1.6, 2.0]$, the velocity correlation increases abruptly at small separations. With increasing separation, the correlation decreases steeply, crossing zero at $L_0 \approx 0.7D$ and becoming anti-correlated at larger separations. With increasing downstream position, the correlation function transitions to lower correlation at small separations and higher correlations at large separations. By $X/D = 3.2$, the correlation profile converges to a shape in which the correlation is high at small separations, reaches a local minimum near $\Delta R/D = 0.3$ and then increases again at larger separations. This observation is surprising and may suggest that the wake has still some memory the inflow, which would explain the high correlation at both small and large separations, while the local minimum marks the turbulence that persists in the shear layer.

Beyond $X/D = 3.6$, the correlation at small separations is high again and decreases gradually up to a separation of $\Delta R/D = 0.6$. At larger separations, it declines more rapidly and reaches zero around $L_0 = 0.9D$. High correlations at small separations are still present up to the furthest downstream measurement location at $X/D = 4.8$ indicating that the wake has not fully decayed to the inflow state at this position, which is not unexpected.

Shear layer Similarly to the core wake, the velocity correlations in the shear layer are high at small separations directly behind the rotor. However, they exhibit a local minimum at a separation of $\Delta R/D = 0.4$ and increase again at the larger separations. With increasing downstream position, the correlations at small separations decline slightly, which may be due to the break down of the tip vortices. However, the high correlations at large separations suggest that coherent structures at the rotor scale are also present.

Similar to the core wake, the velocity correlations at small separations increase abruptly at $X/D \in [1.6, 2.0]$. Over $X/D \in [2.8, 3.2]$, the correlation at small separations is lower than in the core wake, possibly due to the high turbulence level present in the shear layer. Neunaber *et al.* (2020) further identified a region of high intermittency surrounding the wake , which may contribute to reducing the correlations at small separations in this region.

Far downstream of the rotor, at $X/D \in [3.6, 4.0]$, the shear layer correlation profile is similar to the core wake except that it appears to cross zero at a smaller separation of about $L_0 = 0.6D$. This similarity may indicate that the shear layer has extended into the core region.

Outer wake Directly downstream of the rotor, over $X/D \in [0, 1.6]$, L_0 remains roughly around $0.9D$ while the correlation at the smallest scales is strong initially and then decreases progressively, unlike the core wake and shear layer which exhibit an initial drop near $0.5D$. This may be attributed to the absence of wake-generated structures at this downstream distance, even though the outer flow correlation remains influenced by the rotor at small separations.

Over $X/D \in [1.6, 4.0]$, the outer wake exhibits a correlation profile closely similar to the core wake and shear layer, but with higher correlations at small separations far from the rotor. The wake appears to have expanded towards the outer flow. The high correlations persisting over a wide range of separations may be indicative of strong turbulence originating from the growing shear layer. As in the core and shear layer, the flow in this region has not recovered to the inflow state.

CONCLUSION

The radial two-point one-time correlation functions of the rotational velocity component were computed from particle velocities obtained from Lagrangian particle tracking (LPT) at various radial and downstream positions in a wind turbine wake. LPT is shown to provide spatially resolved information about velocity correlation scales that is challenging to acquire using fixed-probe measurements. These data enable the simultaneous characterisation of the core wake, the shear layer, and the outer wake and the interactions between these regions. The results reveal strong variations in correlation scales as a function of downstream and radial position. However, due to the complexity of the interacting flow phenomena, the interpretation of these trends is challenging. Nevertheless, the results show the potential of the two-point one-time radial correlations of the azimuthal velocity component to describe evolution of coherent structures in the wake.

As discussed previously, the particle seeding density in the present study was insufficient to achieve statistical convergence of the correlations at small separations. In future work, the particles will be seeded closer to the rotor to increase the particle density and thus the number of close particle pairs. This will also allow for finer binning in the radial and streamwise dimensions. Finally, additional experiments were conducted in the presence of inflow turbulence, but are not presented here. Future work will use this data toinvestigate how the correlation scales and the identified regions evolve as a function of inflow turbulence.

REFERENCES

Bertens, G., Bagheri, G., Xu, H, Bodenschatz, E. & Moláček, J. 2021 In situ cloud particle tracking experiment. *Review of Scientific Instruments* **92** (12).

Bodenschatz, E., Bewley, G. P., Nobach, H., Sinhuber, M. & Xu, H. 2014 Variable density turbulence tunnel facility. *Review of Scientific Instruments* **85** (9).

Küchler, C., Ibanez Landeta, A., Moláček, J. & Bodenschatz, E. 2024 Lagrangian particle tracking at large reynolds numbers. *Review of Scientific Instruments* **95** (10).

Lawson, John M, Bodenschatz, Eberhard, Lalescu, Cristian C & Wilczek, Michael 2018 Bias in particle tracking acceleration measurement. *Experiments in Fluids* **59** (11), 172.

Miller, M. A., Kiefer, J., Westergaard, C., Hansen, M. OL & Hultmark, M. 2019 Horizontal axis wind turbine testing at high reynolds numbers. *Physical Review Fluids* **4** (11), 110504.

Neunaber, I., Hölling, M., Stevens, R. JAM, Schepers, G. & Peinke, J. 2020 Distinct turbulent regions in the wake of a wind turbine and their inflow-dependent locations: The creation of a wake map. *Energies* **13** (20), 5392.

Placidi, Marco, Hancock, Philip E & Hayden, Paul 2023 Wind turbine wakes: experimental investigation of two-point correlations and the effect of stable thermal stability. *Journal of Fluid Mechanics* **970**, A30.

Porté-Agel, Fernando, Bastankhah, Majid & Shamsoddin, Sina 2020 Wind-turbine and wind-farm flows: a review. *Boundary-layer meteorology* **174** (1), 1–59.